Digital Biomarkers for Diagnosis of Muscle Disorders Using Stimulated Muscle Contraction Signal

Kwangsub Song, Sangui Choi, Jin-Hong Shin, Woo-Hyeon Son, Hyuntae Park, Hooman Lee, *Member, IEEE*, and Nam-Jong Paik

***Abstract*— We propose a digital biomarker related to muscle strength and muscle endurance (DB/MS and DB/ME) for the diagnosis of muscle disorders based on a multi-layer perceptron (MLP) using stimulated muscle contraction. When muscle mass is reduced in patients with muscle-related diseases or disorders, measurement of DBs that are related to muscle strength and endurance is needed to suitably recover damaged muscles through rehabilitation training. Furthermore, it is difficult to measure DBs using traditional methods at home without an expert; moreover, the measuring equipment is expensive. Additionally, because traditional measurements depend on the subjectb's volition, we propose a DB measurement technique that is unaffected by the subjectb's volition. To achieve this, we employed an impact response signal (IRS) based on multi-frequency electrical stimulation (MFES) using an electromyography sensor. The feature vector was then extracted using the signal. Because the IRS is obtained from stimulated muscle contraction, which is caused by electrical stimulation, it provides biomedical information about the muscle. Finally, to estimate the strength and endurance of the muscle, the feature vector was passed through the DB estimation model learned through the MLP. To evaluate the performance of the DB measurement algorithm, we collected the MFES-based IRS database for 50 subjects and tested the model with quantitative evaluation methods using the reference for the DB. The reference was measured using torque equipment. The results were compared with the reference, indicating that it is possible to check for muscle disorders which cause decreased physical performance using the proposed algorithm.**

***Index Terms*— Digital biomarker, diagnosis of muscle disorders, stimulated muscle contraction, impact response signal, multi-frequency electrical stimulation, deep neural network.**

I. Introduction

SKELETAL muscles are essential organs in the human body that consists of contractile tissues [1], [2], [3]. Muscle contraction is responsible for movement during daily activities, and ensures quality of life. Myopathic conditions, including sarcopenia and muscular dystrophy, are accompanied by loss of muscle contractility, which leads to severe weakness. For rehabilitation in patients with muscle disorders due to disease and aging, physiatrists prescribe therapeutic exercise, as well as electrical stimulation [4], [5], [6], [7]. However, patients may have a better chance of recovery if they are diagnosed at an early stage. In addition, it is crucial to monitor the therapeutic effects using unbiased measurements, including assessments of muscle strength (MS) and muscle endurance (ME) [8], [9], [10], [11].

Pharmaceutical companies have developed new drugs for the treatment diseases and disorders, and have conducted clinical tests to prove the efficacy of these drugs. After a patient is prescribed a drug, the patient must periodically visit an institution for its effect to be confirmed through physical checkups. To measure digital biomarkers (DBs) related to the MS and ME (DB/MS and DB/ME), various equipment and scales are used in clinics to evaluate the muscle disorders of patients, for example, torque measurement, timed up and go (TUG) test, five times sit-to-stand test (FTSST), electromyography (EMG), Levettb's test, and Asworthb's scale [12], [13], [14], [15], [16], [17]. Torque measurement and physical scales, including the TUG, FTSST, EMG, Levettb's test, and Asworthb's scale, require time and lead to physical fatigue. Some equipment for measuring torque are large and expensive for personal use, making them unsuitable for use at home.

Manuscript received 25 May 2022; revised 27 September 2022 and 16 January 2023; accepted 24 February 2023. Date of publication 1 March 2023; date of current version 30 March 2023. This work was supported in part by the Korea Medical Device Development Fund funded by the Korean Government (the Ministry of Science and ICT, the Ministry of Trade, Industry and Energy, the Ministry of Health & Welfare, and the Ministry of Food and Drug Safety) under Project 1711138172; in part by the Technology Innovation Program funded by the Ministry of Trade, Industry & Energy (MOTIE), South Korea, under Grant 20015793; and in part by the Seoul National University Bun-Dang Hospital under Grant 14-2018-026. *(Corresponding authors: Hooman Lee; Nam-Jong Paik.)*

This work involved human subjects or animals in its research. Approval of all ethical and experimental procedures and protocols was granted by the Korea Maritime and Ocean University Institutional Review Board under Application No. 1040371-202203-BR-01-02, and performed in line with the guidelines of the Declaration of Helsinki.

Kwangsub Song, Sangui Choi, and Hooman Lee are with the Research and Development Center of Exosystems, Seongnam-si 13449, Republic of Korea (e-mail: will@exosystems.io; tkddml30@exosystems.io; hoomanlee@exosystems.io).

Jin-Hong Shin is with the Department of Neurology, Pusan National University Yangsan Hospital, Yangsan-si 50612, Republic of Korea (e-mail: shinzh@pusan.ac.kr).

Woo-Hyeon Son is with the Division of Navigation Convergence Studies, College of Maritime Sciences, Korea Maritime and Ocean University, Yeongdo-gu, Busan 49112, Republic of Korea.

Hyuntae Park is with the Graduate School of Health Sciences, Dong-A University, Busan 49315, Republic of Korea.

Nam-Jong Paik is with the Department of Rehabilitation Medicine, Seoul National University College Medicine, Seoul National University Bundang Hospital, Seongnam-si 13620, Republic of Korea (e-mail: njpaik@snu.ac.kr).

Digital Object Identifier 10.1109/TNSRE.2023.3250641

In order to continuously receive some drugs, patients who have rare muscle diseases need to undergo periodic checkups to assess the condition of their muscles. To acquire drugs at lower costs, patients must sustain the required condition of their insurance, including undergoing test to determine whether the condition of their muscles improve after the administration of such drugs. However, because it is difficult to measure the patient's condition daily at the hospital, the patient's condition might have been underestimated by external factors when performing a medical checkup at regular intervals. In addition, if the patients can measure the muscle condition at home, misjudgment by underestimation is minimized.

In addition, to reliably check the condition of patients' muscles, patients that require specific clinical tests must visit a research institution, which introduces unnecessary expenses. Hence, to reduce the cost of clinical tests, it is imperative to develop a novel measurement technique to conveniently evaluate DBs related to MS and ME at home. Conventional EMG records the electrical activities of muscle fibers, but EMG cannot be used to measure MS [18]. In addition, the signals from the muscle contraction in conventional EMG are influenced by the patient's volition, which inevitably increases the likelihood of variability in the measurements.

To address these major issues, we obtained stimulated muscle contraction signals called impact response signals (IRS) using a medical device certified by the Ministry of Food and Drug Safety, called the Korea Food and Drug Administration (KFDA). The medical device was equipped with an electrical stimulator and EMG sensor. To record the stimulated muscle contraction signal, while we stimulated the muscle using the medical device, we recorded the EMG signal, i.e., the IRS. Skeletal muscles are composed of type I and type II fibers, which are related to MS and ME, respectively. Type I fibers are slow-twitch fibers that are resistant to muscle fatigue, and are closely related to exercise endurance. Type II fibers are fast-twitch fibers that can produce powerful contractions but are vulnerable to fatigue. The fibers are related to MS [19], [20], [21]. Therefore, we stimulated the muscle to obtain biomedical information that correspond to these two characteristics. The stimulated muscle contraction signal depends on the electrical stimulation frequency parameter. Furthermore, to comprehensively analyze the muscle characteristics, we collected the multi-frequency IRS (m-FIRS), which included the IRS recorded by the electrical stimulation set using various frequency parameters. The proposed algorithm employs the m-FIRS recording method to estimate the DB using an artificial intelligence model based on a multi-layer perceptron (MLP) to measure the DB/MS and DB/ME. In addition, to determine the reference value for the m-FIRS, we measured DB/MS and DB/ME using equipment for isokinetic systems, under guidance of a medical professional. Because the m-FIRS may be contaminated by muscle fatigue, we first measured the m-FIRS and then collected the reference values using isokinetic equipment.

Our approach in this study was to estimate DB/MS and DB/ME using an MLP model with a medical device. Therefore, we first recorded the m-FIRS using the medical device, and the signal was passed through the preprocessing algorithm to suppress the artifacts caused by the electrical stimulation. To extract a feature for the measurement of DB/MS and DB/ME, we extracted a feature vector from the m-FIRS and suppressed the noise signal. Therefore, we analyzed the frequency components of the m-FIRS and extracted the feature vector to manifest the variation in the muscle contraction while changing the frequency parameter of the electrical stimulation. We also analyzed the temporal components of m-FIRS and extracted the time domain feature vector. When all the features are employed as the input of the MLP model, overfitting may occur because of the large size of the feature vector. Hence, we performed feature selection to reconstruct the extracted input vector to estimate the DB in order to improve the performance of the technique. Thus, to select the features correlated with the DB/MS and DB/ME, we analyzed the Pearson correlation of the features. Finally, we extracted the feature vector for the MS and ME, and fed the feature vector to the MLP model to estimate the DB.

Finally, we trained the classification and regression models using the MLP scheme to train the MLP model to estimate the DB. We evaluated the performance of the proposed algorithm by comparing it with a conventional machine-learning method. In addition, to evaluate the performance of the proposed algorithm, we conducted an n-fold cross-validation. Further, after the m-FIRS was collected through a medical device called ExoRehab, the signal was transmitted to a mobile device via Bluetooth. Subsequently, the DB/MS and DB/MS were measured using the MLP model on the mobile device. Because our technique does not require patientsb' voluntary movements during measurements, it provides unbiased measurements. Therefore, the proposed DB measurement method can be adopted as an objective method for muscle evaluation. In short, our technique does not depend on the subject's volition since we only used stimulated muscle contraction signal without voluntary muscle contraction caused by the subject's voluntary action.

In addition, our technique can be used conveniently in home care settings without trained personnel. Furthermore, the production cost of conventional equipment for measuring torque, such as Biodex is high because the equipment is huge. Moreover, because it is difficult to produce the equipment in large quantities, the unit price of each equipment is often high. However, the production cost of our device is much lower than that of conventional equipment owing to its small size. The unit price of our device is also low because mass production is possible. Hence, it is possible to check the DB using our system at home.

This paper is further organized as follows: The proposed algorithm is described in section II. Section III presents the results of the study. Section IV presents a discussion, and Section V concludes the paper. The acronyms used are listed in Table I.

II. Methods

A. Concept of Proposed Algorithm

Myofibrils are composed of myosin and actin filaments, and are a major component of muscle fibers. Muscle contraction occurs when the myofibril interval is narrowed by crosslinking between filaments. The quantity of myofibrils is correlated

TABLE I
LIST OF ACRONYMS

Acronym	Meaning
DB	digital biomarker
TUG	timed up-and-go test
FTSST	five times sit-to stand test
EMG	electromyography
IRS	impact response signal
m-FIRS	multifrequency IRS
MLP	Multi-layer perceptron
LCC	level crossing counting
PoSCS	percentile of spectral cumulative sum
SBPE	spectral band power envelope
SCS	spectral cumulative sum
ELU	exponential linear unit
AUC	area under the receiver operating characteristic curve
SVM	support vector machine
GMM	Gaussian mixture model
ANN	artificial neural network
SNR	signal-to-noise ratio
MSE	mean square error
CoV	coefficient of variation

with the tension that the muscle fibers can produce. Therefore, the amount of myofibrils must be increased to improve MS.

Muscles were made to contract involuntarily using electrical stimulation. IRS data were then collected using an EMG sensor to record the muscle contraction. Type I and type II fibers bionically responded to the electrical stimulation, and biomedical information was captured using an EMG sensor. The proposed algorithm consists of a stimulated muscle contraction signal and an MLP model that estimates DB/MS and DB/ME. The stimulated muscle contraction signal was defined as electricalb-physiological data, and we employed electrical stimulation with various frequency parameters to search for biomedical information from the signal. Therefore, we expected that the proposed algorithm would electricallyb-physiologically estimate biomedical information, such as DB/MS and DB/ME.

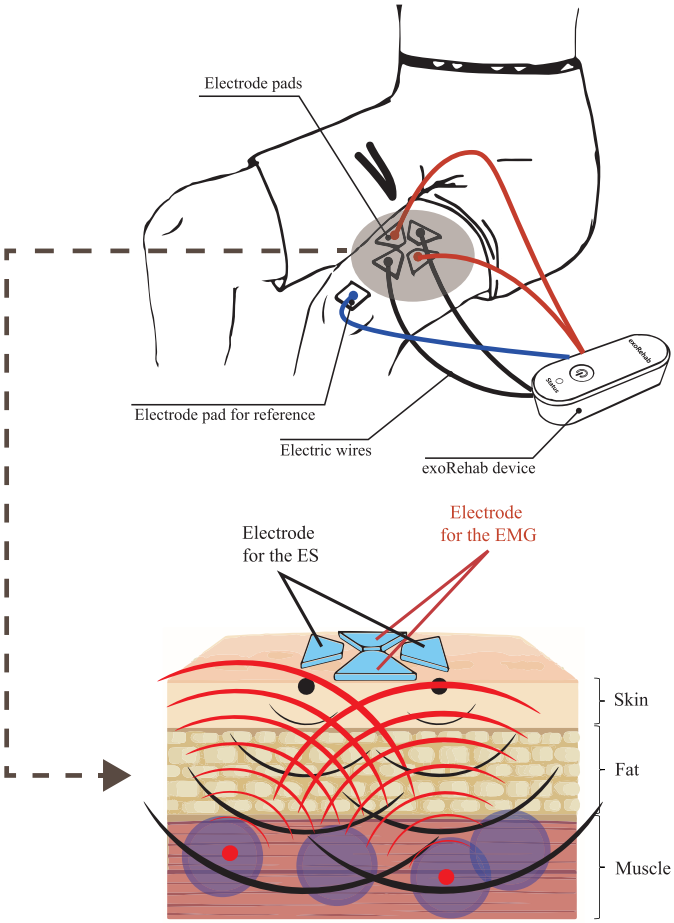

Fig. 1. Outline of the m-FIRS data-acquisition method. The red, yellow, and blue wires are the electrodes for the EMG, electrical stimulation, and reference of the EMG sensor, respectively. The figure shows the concept of IRS data collection. While the electrical stimulation stimulates the muscle, the muscle response signal is captured by the EMG sensor, as indicated by the blue arrow line.

B. Biomedical Signal and Preprocessing

In this section, we describe the DB measurement algorithm based on the MLP model using m-FIRS. We used five electrodes connected to the medical device via an extension line, and electrode pads were connected to each electrode. Two electrodes were used to generate the electrical stimulation and two electrodes were used to record the EMG signals. The remaining electrode functioned as the reference electrode. To record the m-FIRS, electrode pads connected to the device were attached to the target muscle (thigh), as shown in Fig. 1. Finally, while we stimulated the skeletal muscle of the thigh using the electrical stimulation device, we recorded a biomedical data signal called the m-FIRS using an EMG sensor. The electrical stimulation frequency parameter was set to 10, 15, 20, 25, and 30 Hz, and then the IRSs were collected for each frequency in a sequence. Initially, to measure the DB, preprocessing was performed to remove artificial noise, such as electrical stimulation, as shown in Fig. 2. Since we design the muscle contraction signal which involuntarily occurs after electrical stimulation, the other signal except for the muscle contraction signal was defined as noise. In addition, because the noise signal may negatively affect the output of the feature extraction procedure, preprocessing was required in order to improve the performance of the proposed algorithm.

Therefore, because the m-FIRS was obtained from the EMG sensor while the muscle was subjected to electrical stimulation, the signal was contaminated by artificial noise. The noise signal made it difficult to analyze m-FIRS, and the performance of the proposed algorithm was degraded by the noise signal. Thus, we applied a preprocessing method to suppress the artificial noise signal using label data, where the medical device recorded the time information when the electrical stimulation occurs. Finally, the suppressed EMG signal y was obtained as follows:

$$y(t+i) = (x(t+i-2) + x(t+i-1) + x(t+i) + x(t+i+1) + x(t+i+2))/5, 1 \le i \le 15 \quad (1)$$

where t and i are the time and filter sliding indices, respectively, and x represents the input EMG signal. The preprocessing method employs a moving averaging filter on the order of five, and the method is iteratively applied to 15 samples after electrical stimulation occurs. Because the artificial signal appeared prominently until after 15 samples, we iteratively applied the filter to 15 samples. The parameter of moving

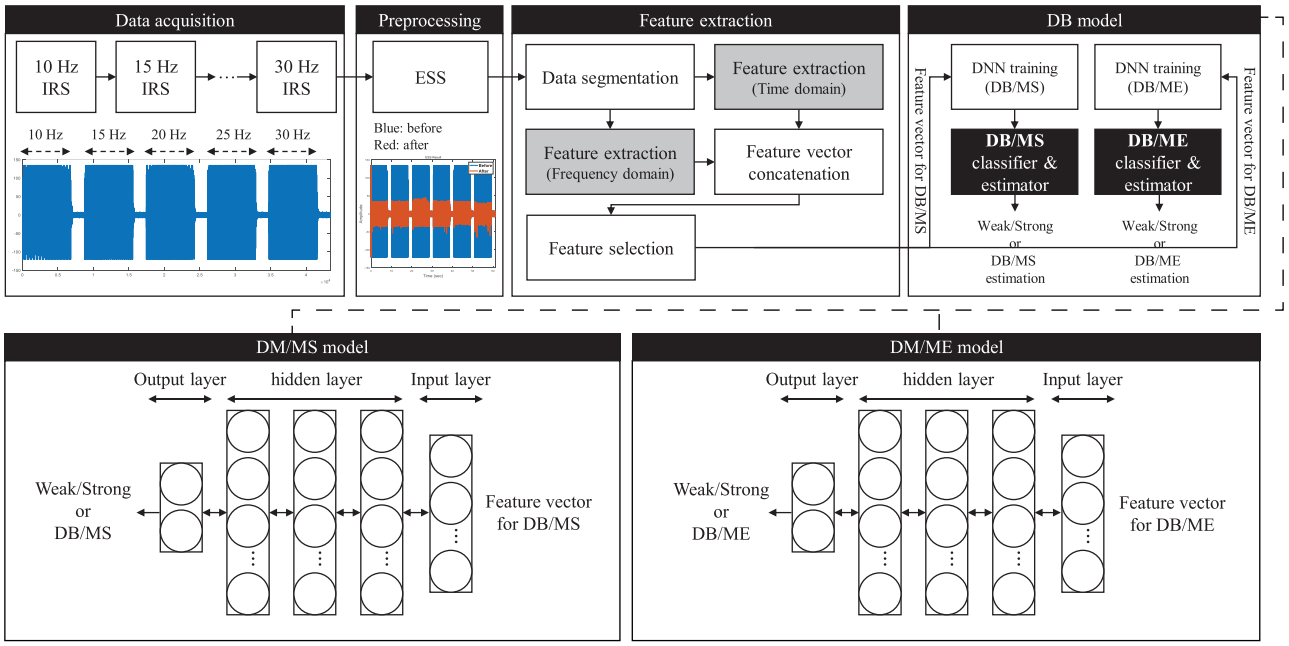

Fig. 2. Block diagram of the proposed algorithm.

TABLE II
SUMMARY OF FEATURE VECTOR TO EXTRACT THE MUSCLE CONDITION. ABBREVIATIONS; LEVEL CROSSING COUNTING (LCC), PERCENTILE OF SPECTRAL CUMULATIVE SUM (POSCS), STATISTIC (STAT), SPECTRAL BAND POWER ENVELOPE (SBPE)

Item	Time domain	Frequency domain
1	Power pattern	PoSCS
2	Power variance	PoSCS-STAT
3	LCC pattern	SBPE
4	-	SBPE-GAP

averaging filter were empirically determined to extract the feature vector which entirely had high correlation with reference. Since we needed to extract high correlation features to train the best performance model, the filter length and iteration number were determined with five and fifteen.

C. Feature Extraction

To determine the characteristics of the muscle using m-FIRS, we extracted the feature vector from the stimulated muscle contraction signal, where the artificial noise was suppressed. Two types of features (time-domain and the frequency-domain features) were used to extract the feature vector, as shown in Table II. We also extracted the feature vector from the IRS for each frequency and extracted additional feature vectors using the integrated m-FIRS, which concatenated each IRS sequentially. In the time-domain feature-extraction step, we first extracted the power pattern PP(n) and variance PV as follows:

$$\mathrm{PP}(n) = \sum_{t=0}^{T_n} |y_n(t)|, \quad \text{for } 1 \le n \le 5 \tag{2}$$

where n is the index of the frequency parameter, that is, 10 Hz, 15 Hz, ..., 30 Hz. In Addition, T_n represents the length of the input signal. We extracted the variance PV of the power pattern vector. Thus, we can obtain the variation features of the energy of the stimulated muscle contraction in accordance with the electrical stimulation frequency using PP(n) and PV.

We extracted the level crossing counting (LCC) pattern LP(n) for the m-FIRS as follows:

$$\mathrm{LP}(n) = \sum_{t=1}^{T_n} (s(t) - s(t-1)), \quad \text{for } 1 \le n \le 5 \tag{3}$$

$$s(t) = \begin{cases} 1 \text{ if } (y_n(t) - \alpha) > 0 \\ 0 \text{ if } (y_n(t) - \alpha) \le 0 \end{cases} \tag{4}$$

where $s(t)$ indicates a positive or negative sign of $y_n(t) - \alpha$, and α represents a constant that is a natural number between 1 and 30. The maximum amplitude of $y_n(t)$ is expressed until almost 30-40; therefore the constant value is determined to be between 1 and 30. Furthermore, because the characteristic of the muscle that responds minutely to electrical stimulation is expressed in the IRS, we calculated the LCC with an increase in α to investigate the minute movement of the muscle.

In the frequency-domain feature-extraction step, $y_n(t)$ is transformed into frequency data in the discrete Fourier transform domain $Y_n(k)$, where k represents the index of the frequency bin. First, we extracted the percentile of the spectral cumulative sum (PoSCS) PoSCS(a_1) using $Y_n(k)$ as follows:

$$\mathrm{PoSCS}_n(a_1) = \mathrm{argmin}(|f_n - 0.01a_1|), \quad \text{for } 1 \le a_1 \le 95,\ 1 \le n \le 5 \tag{5}$$

$$f_n(k) = \frac{1}{f_n(K-1)} \sum_{m=0}^{k} Y_n(m), \quad \text{for } 0 \le k < K,\ 1 \le n \le 5 \tag{6}$$

where m and a_1 are indices of the frequency bin and horizontal lines, respectively. In addition, $f_n(k)$ denotes the function

of the spectral cumulative sum (SCS), and K was set to 4096. We can analyze the variation in the muscle that reacts with the electrical stimulation in terms of the frequency data through the function of the SCS; therefore it is possible to observe the frequency response of the muscle at a specific percentile of the total energy in the frequency domain. At this time, the input length for extracting all features was set to 6800 samples to analyze each IRS entirely. Hence, to analyze the statistical properties of the muscle variation in accordance with time variation, we extracted PoSCS-STAT $\mathrm{PoS}_{n,\mu}(a_2)$, $\mathrm{PoS}_{n,\sigma}(a_2)$ using m-FIRS. We first calculated the PoSCS pattern $\mathrm{PoP}_n(a_2, j)$ as follows:

$$\mathrm{PoP}_n(a_2, j) = \mathrm{argmin}(|f_{n,j} - 0.05a_2|), \quad \text{for } 1 \le a_2 \le 19,\ 1 \le j \le 8,\ 1 \le n \le 5 \tag{7}$$

where j and a_2 represent the frame and horizontal line indices, respectively. To extract $\mathrm{PoS}_{n,\mu}(a_2)$ and $\mathrm{PoS}_{n,\sigma}(a_2)$, we calculated the average μ and standard deviation σ of $\mathrm{PoP}_n(a_2, j)$ as follows:

$$\mathrm{PoS}_{n,\sigma}(a_2) = \sqrt{\frac{1}{7}\sum_{j=1}^{8}(\mathrm{PoP}_n(a_2, j) - \mathrm{PoS}_{n,\mu}(a_2))^2}, \quad \text{for } 1 \le a_2 \le 19,\ 1 \le n \le 5 \tag{8}$$

$$\mathrm{PoS}_{n,\mu}(a_2) = \frac{1}{8}\sum_{j=1}^{8}\mathrm{PoP}_n(a_2, j), \quad \text{for } 1 \le a_2 \le 19,\ 1 \le n \le 5. \tag{9}$$

$\mathrm{PoP}_n(a_2, j)$ was extracted from the f_n of each frame, and then we calculated μ and σ to investigate the statistical characteristics of each PoSCS for all the frames. Additionally, because each IRS of the m-FIRS was recorded for 8 s through the EMG sensor, the number of frames for each IRS was eight.

$$\mathrm{SE}_n(j) = \log\Big(\sum_{k=0}^{b_1}|Y_n(j,k)|, \sum_{k=b_1+1}^{b_2}|Y_n(j,k)|, \ldots, \sum_{k=b_4+1}^{b_5}|Y_n(j,k)|\Big),\ 1 \le j \le 8,\ 1 \le n \le 5 \tag{10}$$

where $b_1, \ldots,$ and b_5 are the frequency indices of the band. The frequency range was divided equally into five bands. To measure the activity volume of each frequency band over time, we extracted SBPE for each IRS. We recorded the EMG signal while stimulating the muscle using electrical stimulation, and the data were repeatedly recorded for various electrical stimulation, where the frequency parameter was set to 10 Hz, 15 Hz, ..., 30 Hz. To extract the change in activity volume between the IRSs, we calculated SBPE-GAP $\mathrm{SG}(l)$ as follows:

$$\mathrm{SG}(l) = \mathrm{SE}_{l+1} - \mathrm{SE}_1, \quad \text{for } 1 \le l \le 4 \tag{11}$$

where l denotes feature index. $\mathrm{SG}(l)$ indicates the variation between two IRSs and implies the changed activity volume of the muscle when the electrical stimulation for 10 Hz is compared with that of other frequencies. Finally, we extracted the features including PoSCS, PoSCS-STAT, SBPE, and SBPE-GAP using the integrated m-FIRS, and all of the features were concatenated into one vector to employ the input of the deep-learning model. In addition, the m-FIRS was collected five times per subject, and average of each feature of the vectors extracted for the five data were used as the input of the MLP model. Afterwards, the feature vector was reconstructed using the feature-selection procedure, where we select features that have a high correlation coefficient with the reference. At this time, as shown in Fig. 2, because the MLP models for estimating the DB/MS and DB/ME were trained, each feature vector for the DB/MS and DB/ME were reconstructed by feature selection in accordance with the MS and ME labels, respectively.

D. Model Training

Although the features were extracted from the m-FIRS, which includes biomedical information for the DB, it was difficult to estimate the DB/MS and DB/ME using only the feature vector without the MLP model. In particular, we had to train the model to robustly estimate the DB indicators related to MS and ME using the feature vector. Therefore, we respectively trained two MLP models to estimate the DB/MS and DB/ME as shown in Fig. 2.

The MLP model consists of three or more hidden layers and two or more hidden unit between the input layer and output layer, and the hidden layer and hidden unit are expressed with the weight matrix and bias vector. Furthermore, the MLP architecture which emulates the human brain enables efficient modeling of complicated non-linear relationship data. Hence, for modeling data consisting of our complex features, we trained the estimation model using the MLP architecture. For the MLP model learning, the feature vector was normalized using the mean and standard deviation of each feature. This required two stages: the model parameter initialization stage and a fine-tuning stage to train the MLP model for DB indicators. In the MLP parameter initialization stage, we randomly initialized the model parameters of the hidden layers with a uniform distribution (mean of 0) and then fine-tuned them using a backpropagation technique. In the backpropagation scheme, the model parameters obtained at the initialization stage are updated. To do this, the exponential linear unit (ELU) function $g(x)$ was used as an activation function for the MLP model, and it was given as

$$g(x) = \begin{cases} x & x \ge 0 \\ \gamma(e^x - 1) & x < 0 \end{cases} \tag{12}$$

where x denotes the index of the activation function and γ is the parameter of the function, which is set to 1. The parameters, including the weight matrix and bias vector, were updated at each layer of the model based on the binary cross-entropy loss function [22]. To do this, the binary cross-entropy loss function L was defined as

$$L = -\frac{1}{M}\sum_{m=1}^{M}[Q_m \ln(\hat{Q}_m) + (1 - Q_m)\ln(1 - \hat{Q}_m)] \tag{13}$$

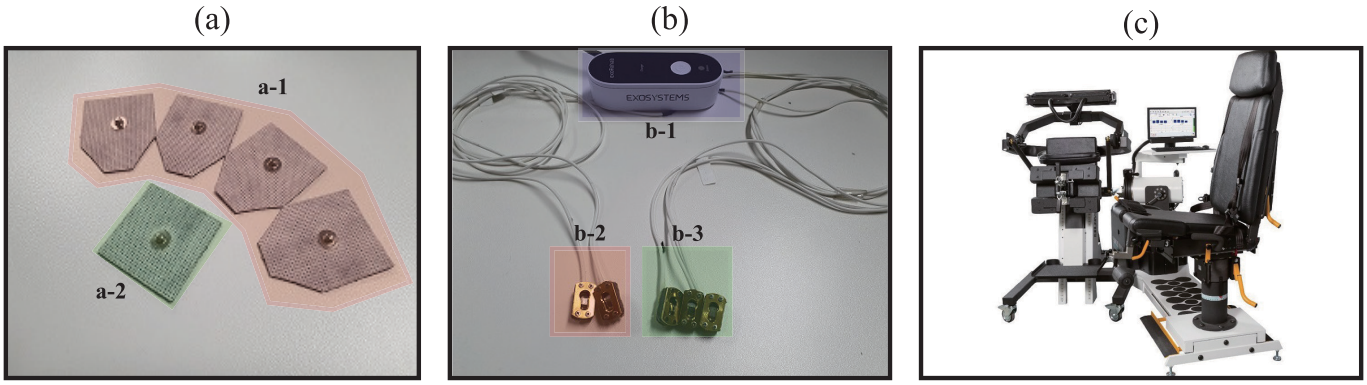

Fig. 3. Experimental equipment. (a) Electrode pads: (a-1) electrode pads for the electrical stimulation and EMG sensor; (a-2) electrode pad for the reference. (b) Device for the electrical stimulation: (b-1) ExoRehab (sensing device); (b-2) electrode for the electrical stimulation; (b-3) electrode for the EMG; (c) torque equipment for the hospital.

where m and M represent the index and the size of the mini-batch, respectively. Additionally, Q_m and $\hat{Q}_m$ denote the DB reference and prediction results of the trained MLP model, respectively. Subsequently, the parameters are repeatedly updated using adaptive moment estimation to optimize the model [23]. Finally, the MLP learning procedure is repeated for a high-performance model until a specific epoch, after which the model classifies the weak and strong in terms of MS O_{str} and ME O_{end} as follows:

$$O_{\text{str}} = g(g(g(Q_{\text{str}}w_{1,\text{str}} + b_{1,\text{str}})w_{2,\text{str}} + b_{2,\text{str}})w_{3,\text{str}} + b_{3,\text{str}})w_{\text{o,str}} + b_{\text{o,str}} \quad (14)$$

$$O_{\text{end}} = g(g(g(Q_{\text{end}}w_{1,\text{end}} + b_{1,\text{end}})w_{2,\text{end}} + b_{2,\text{end}})w_{3,\text{end}} + b_{3,\text{end}})w_{\text{o,end}} + b_{\text{o,end}} \quad (15)$$

where Q_{str} and Q_{end} are the feature vectors for DB/MS classifier and DB/ME, respectively. w denotes the weight matrix, and b denotes the bias vector. To estimate the O_{str} and O_{end} with the model parameters, we first multiplied the normalized feature vector and weight matrix of the first hidden layer, and added the multiplication result and bias vector of the first hidden layer. Subsequently, the sum of the bias vector of the first hidden layer and the multiplication result passes through the ELU function. Because the number of hidden layers was set to three, the calculation procedure was repeated three times until the third layer was reached. In the output layer, the output value is calculated without the ELU function. Finally, DB/MS and DB/ME were classified in terms of weakness and strength according to the threshold.

III. Result

A. Statistics

To evaluate the performance of the proposed algorithm, we first trained a classification model based on MLP that distinguished weak from strong in terms of DB/MS and DB/ME. We trained a regression model to estimate the quantitative value of the reference for DB/MS and DB/ME. To validate the performance of the classification model based on MLP, we employed a confusion matrix, the area under the receiver operating characteristic curve (AUC), and a boxplot between the classification result and the reference value. In addition, the regression models were validated using the Pearson correlation coefficient r between the regression results and the reference values. Finally, we compared the proposed algorithm with conventional algorithms, including a support vector machine (SVM), Gaussian mixture model (GMM), and an artificial neural network (ANN), using measurements for performance evaluation. All statistical analyses were performed using MATLAB R2020b software.

B. Data Collection Protocol and Data Sets

All participants signed an informed consent form before data collection. For the experiment involving the DB measurement algorithm shown in Fig. 3, we employed a medical device (ExoRehab, Exosystems, Seongnam, Gyeonggi-do, Republic of Korea), which was installed in the electrical stimulation generator and was approved as a medical device by the Korean government. In addition, we used electrode pads [width: 60 mm, height: 44 mm; contact surface component: hydrogel; resistance: 50 Ω per 20 mm] (StiMus Electrode, HUREV Corp., Wonju, Gangwon-do, Republic of Korea), as shown in Fig. 3. Because the DB measurement technique had to be applied in the ExoRehab device, the electrode pads were cut in a manner similar to the planned commercialization product.

To collect the database for the DB experiment, we collected data, including m-FIRS and its reference, verified by experts at a medical center, including a veteran medical doctor team from one of the best hospitals (Asan Medical Center) in Korea. To record the m-FIRS, we attached electrode pads to the right thigh of the subject, as shown in Fig. 1. The IRS was recorded using the EMG sensor for 8 s while the muscle was stimulated using the electrical stimulation generator, as shown in Fig. 4, and it was additionally recorded with the electrical stimulation set to another frequency after 2 s of rest. In addition, to collect m-FIRS data using a varying frequency, which was set from 10 to 30 Hz, we repeatedly recorded the data while increasing the parameter by 5 Hz. The amplitude of the electrical stimulation was set to 22.10, at which point the subject could endure the pain of electrical stimulation. Afterwards, to construct the labeled database for the DB experiment, the m-FIRS reference was labeled by a medical doctor at the

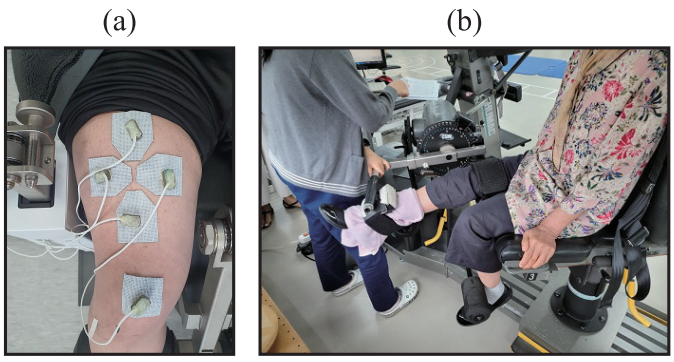

Fig. 4. Photographs of m-FIRS collection. (a) Scene for recording the m- FIRS. (b) Scene for recording the reference.

medical center using a torque equipment (HUMAC NORM, CSMi, Stoughton, Massachusetts, US), as shown in Fig. 3. The labeling procedure for interested readers is summarized in Appendix A. Finally, we collected the labeled database (DB/MS: 95.4 ± 30.6, DB/ME: 0.18 ± 0.08), which consisted of 50 subjects (weight: 57.3 ± 7.0 kg, age: 71.6 ± 6.6) at the medical center.

To evaluate the performance of the proposed algorithm, we performed n-fold cross-validation. After the reference that was labeled by the torque data was sorted in ascending order, each data point, including the m-FIRS and the reference, was assigned in sequence for the three groups. The DBs of the two groups were employed to train the model, and the performance of the proposed algorithm was evaluated using the remaining group. Thus, the test database did not include the training database, and we conducted the experiments the three times according to three combinations to construct two training groups and one test group.

C. Preprocessing and Data Analysis

While subjecting the muscle to electrical stimulation, we recorded the EMG signal to obtain the IRS. However, the EMG signal was contaminated by the electrical stimulation, and the noisy signal degraded the performance of the proposed algorithm. Thus, to suppress artifact noise due to electrical stimulation, the EMG signal was passed through the preprocessing procedure, as shown in Fig. 2. When we applied the preprocessing method described in Section II-A, we confirmed that artificial noise with an average signal-to-noise ratio (SNR) of -12 dB was removed, as shown in Fig. 5. To calculate the SNR of the noisy signal, the epoch length was set to 1000 samples from the front. After applying preprocessing, we can obtain a stimulated muscle contraction signal that does not include the electrical stimulation. Although we expected that the stimulated muscle contraction signal would be different for each subject according to the characteristics of the muscle, it was difficult to estimate the DB using the waveform without the data analysis technique. Therefore, to estimate the DB using the MLP model, we extracted features from the m-FIRS using the signal analysis technique described in Section II-B.

The extracted features were employed as the input of the MLP model for estimating the DB, and each feature had

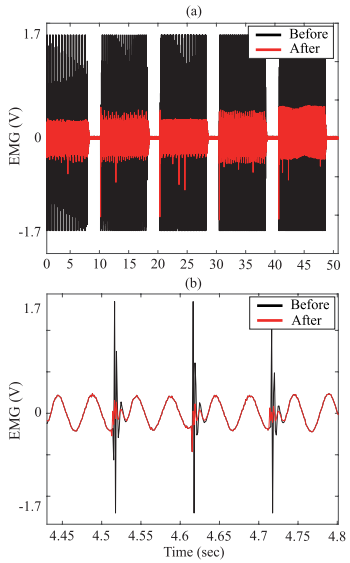

Fig. 5. Experimental results for the preprocessing procedure: (a) entire m-FIRS waveform; (b) magnified m-FIRS waveform.

to represent the correlation between the features and the reference to robustly estimate the DB, as shown in Fig. 6. In addition, because the dimension of the feature vector was too large, it may have caused the curse of dimensionality, and degraded the model's performance. Hence, to alleviate the overfitting problem, we reconstructed the feature vector using the correlation coefficient between the features and the reference. Because the fair correlation coefficient was defined as ± 0.3 [24], the features between which the coefficient was ± 0.3 were selected for the training database. Moreover, since three training database sets were constructed by the three-fold cross validation, each feature vector for the three training database sets was differently constructed after the feature selection. To select common feature vector for three-fold cross validations, the intersection of the feature by voting approach was then finally determined as the feature vector for the input of the MLP model. Also, the input length for DB/MS model and input length for DB/ME model were set to 241 and 151 after the feature selection procedure. At this time, the procedure for feature selection were carried out with training set only. Thus, each feature vector for the two DB elements was determined through the procedure. The absolute coefficient r between the features and reference is presented in Table III. As shown in Fig. 6, the coefficients of the specific feature were 0.63 in terms of the DB/MS in the training database, and the coefficients of other features for the DB/ME were 0.55 in the training database. As a result, when we analyzed the results for the coefficient, we found that the selected features moderately expressed the DB reference.

D. DB Estimation

To validate the proposed algorithm, we compared it with conventional methods including SVM, GMM, and ANN. We then evaluated the performance of the classification models through objective measurements and trained the regression models to verify the feasibility of the proposed algorithm

TABLE III
EXPERIMENTAL RESULTS OF THE CORRELATION COEFFICIENT BETWEEN THE REFERENCE AND FEATURE

		Correlation between muscle strength and feature						Correlation between muscle endurance and feature					
		Time domain feature		Frequency domain feature				Time domain feature		Frequency domain feature			
Set no.	Meas	Power pattern, var	LCC pattern	PoSCS	PoSCS -STAT	SBPE	SBPE -GAP	Power pattern, var	LCC pattern	PoSCS	PoSCS -STAT	SBPE	SBPE -GAP
Set1	AVG	0.32	0.32	0.32	None	0.32	0.38	0.32	0.35	0.36	0.35	0.30	0.39
	STD	0.00	0.01	0.02	None	0.00	0.07	0.08	0.04	0.04	0.06	0.00	0.08
	MAX	0.32	0.33	0.35	None	0.32	0.58	0.32	0.45	0.45	0.46	0.30	0.55
Set2	AVG	0.40	0.32	0.36	0.33	0.34	0.40	0.35	0.36	0.33	0.34	0.32	0.34
	STD	0.06	0.01	0.05	0.03	0.03	0.07	0.02	0.04	0.04	0.04	0.02	0.04
	MAX	0.44	0.34	0.51	0.36	0.39	0.63	0.36	0.44	0.43	0.42	0.36	0.42
Set3	AVG	0.37	0.38	0.37	0.39	0.37	0.38	0.44	0.33	0.30	0.34	None	0.37
	STD	0.04	0.05	0.04	0.04	0.05	0.02	0.00	0.01	0.00	0.03	None	0.08
	MAX	0.45	0.49	0.49	0.51	0.53	0.40	0.44	0.34	0.30	0.39	None	0.56

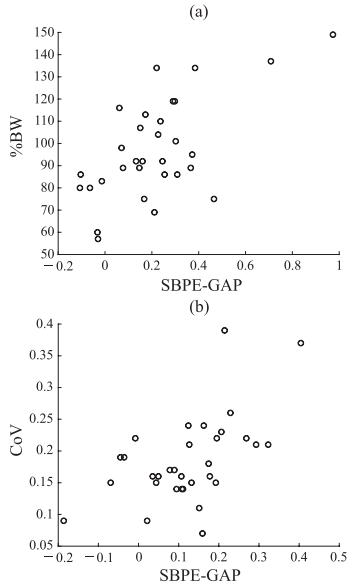

Fig. 6. Relationship between the reference value and feature. (a) Comparison of the DB/MS and SBPE-GAP. (b) Comparison of the DB/ME and SBPE-GAP.

to quantitatively estimate the reference. To classify the DB, we trained the classification model based on the MLP technique described in Section II-C. The number of hidden layers was set to three, and the number of hidden units was set to [256, 256, 256]. In addition, to alleviate the overfitting problem, a dropout set of 0.5 was applied, and we employed L2 regularization when training the model. Since SVM model can outstandingly classify non-linearly separable dataset in feature space using kernel function, it was frequently employed in these machine learning field [25], [26]. Because SVM-based model might show higher performance than the MLP model by the merit of SVM, we compared the SVM model with the MLP model. To train the SVM model, we selected a third-order polynomial function for kernel function, and the kernel scale was automatically searched for log-scaled positive values in the range of [0.001, 1000]. The kernel function was determined through extensive experiments to determine the optimal model performance. GMM was a soft clustering approach, and each data was expressed with probability belonged to each cluster. GMM was defined by probabilistic model that assumed all data were generated from a mixture of a finite number of Gaussian distributions. In addition, GMM algorithm showed superior results even if training database was comparatively small [27], [28]. Hence, we verified the GMM model whether it showed high performance than MLP model. Thus, to train the GMM model, the number of mixtures for the strong and weak classes was set to eight and eight, respectively. To verify the neural network based on single hidden layers, we employed the ANN model [29], [30]. The number of hidden layers affected the performance, and the number of hidden layer was set to three in order to present the best performance in MLP model. The MLP performance was improved according to increasing the number of hidden layers, but overfitting issue occurred by the too much layers. However, although we found the optimal parameter for MLP, we evaluated the performance of ANN model in order to definitely verify performance gap between the multi-layer and single layer. To learn the ANN model, the number of units was empirically determined to be 256, and the model parameter of the ANN model was updated using the loss function called the binary cross-entropy. In addition, the dropout was set to 0.5 to minimize the overfitting, and L2 regularization was applied to optimize the model. Finally, we used the same features extracted from the training database to evaluate both conventional model and MLP model. The parameters of the conventional and MLP models were empirically determined through extensive experiments to optimize performance.

We conducted a performance evaluation using the test database for the models; the experimental results are presented in Tables IV and V. The proposed model based on the MLP technique outperformed the conventional model in terms of objective measurements. In addition, when the performance was evaluated through a three-fold cross validation, as shown in Tables IV and V, the results for all validations indicated that the proposed model robustly estimated the DB/MS and DB/ME better than the conventional model. Although the DB model classifies strong and weak DB elements, the elements cannot be distinguished using the classification model based on MLP. Hence, to confirm the feasibility of quantitative measurement, we trained the regression model based on MLP to estimate the reference value that was labeled by the expert using the torque equipment in the medical center. The loss function for the regression DB model was replaced with the mean squared error (MSE) function, which is typically employed in the MLP model for the regression task.

TABLE IV

CLASSIFICATION MODELS PERFORMANCE FOR THE DB/MS. ABBREVIATIONS; EXPERIMENTAL (EXP), REFERENCE (REF), ESTIMATION (EST)

Item			Conventional model						Proposed model	
Exp no.	Meas.		SVM		GMM		ANN		MLP	
			Strong	Weak	Strong	Weak	Strong	Weak	Strong	Weak
Set1	CM	Strong	66.7%	33.3%	66.7%	33.3%	83.3%	16.7%	100.0%	0.0%
		Weak	18.2%	81.8%	36.4%	63.6%	30.8%	69.2%	7.7%	92.3%
	AUC		0.68		0.64		0.81		0.94	
	Total accuracy		76.5%		64.7%		73.7%		94.7%	
Set2	CM	Strong	50.0%	50.0%	66.7%	33.3%	83.3%	16.7%	100.0%	0.0%
		Weak	33.3%	66.7%	25.0%	75.0%	15.4%	84.6%	7.7%	92.3%
	AUC		0.53		0.65		0.85		0.99	
	Total accuracy		61.1%		72.2%		84.2%		94.7%	
Set3	CM	Strong	33.3%	66.6%	50.0%	50.0%	66.7%	33.3%	100.0%	0.0%
		Weak	8.3%	91.7%	25.0%	75.0%	0.0%	100.0%	8.3%	91.7%
	AUC		0.39		0.47		0.82		0.93	
	Total accuracy		72.2%		66.7%		89.5%		94.4%	
Total average	Averaged sensitivity		50.0%		61.1%		77.8%		100.0%	
	Averaged specificity		80.1%		71.2%		84.6%		92.1%	
	Averaged AUC		0.53		0.59		0.83		0.95	
	Total accuracy		69.9%		67.9%		82.5%		94.6%	

TABLE V

CLASSIFICATION MODELS PERFORMANCE FOR THE DB/ME. ABBREVIATIONS; EXPERIMENTAL (EXP), REFERENCE (REF), ESTIMATION (EST)

Item			Conventional model						Proposed model	
Exp no.	Meas.		SVM		GMM		ANN		MLP	
			Strong	Weak	Strong	Weak	Strong	Weak	Strong	Weak
Set1	CM	Strong	50.0%	50.0%	55.6%	44.4%	75.0%	25.0%	87.5%	12.5%
		Weak	66.7%	33.3%	37.5%	62.5%	11.1%	88.9%	0.0%	100.0%
	AUC		0.39		0.51		0.81		0.94	
	Total accuracy		58.8%		58.8%		82.4%		94.1%	
Set2	CM	Strong	72.7%	7.3%	85.8%	14.2%	71.4%	28.6%	100.0%	0.0%
		Weak	8.6%	71.4%	36.4%	63.6%	9.1%	90.9%	9.1%	90.9%
	AUC		0.66		0.82		0.83		0.91	
	Total accuracy		72.2%		72.2%		83.3%		94.4%	
Set3	CM	Strong	62.5%	37.5%	60.0%	40.0%	100.0%	0.0%	100.0%	0.0%
		Weak	20.0%	80.0%	62.5%	37.5%	50.0%	50.0%	0.0%	100.0%
	AUC		0.61		0.61		0.80		1.00	
	Total accuracy		72.2%		66.7%		77.8%		100.0%	
Total average	Averaged sensitivity		61.7%		67.1%		82.1%		95.8%	
	Averaged specificity		61.6%		54.5%		76.6%		97.0%	
	Averaged AUC		0.55		0.65		0.81		0.95	
	Total accuracy		67.7%		65.9%		81.2%		96.2%	

TABLE VI

MLP-BASED REGRESSION MODEL PERFORMANCE FOR THE DB/MS AND DB/ME. ABBREVIATIONS; MEASUREMENT (MEAS), AVERAGE ERROR (AE), ERROR STANDARD DEVIATION (ESTD)

Meas.	Set1	Set2	Set3	Average
DB/MS r	0.74	0.70	0.71	0.72
DB/MS AE $\pm$ ESTD	-0.62 $\pm$ 14.20	1.99 $\pm$ 18.41	1.29 $\pm$ 16.32	0.89 $\pm$ 16.31
DB/ME r	0.71	0.70	0.71	0.71
DB/ME AE $\pm$ ESTD	0.03 $\pm$ 0.03	-0.01 $\pm$ 0.06	0.03 $\pm$ 0.06	0.02 $\pm$ 0.05

Consequently, the MLP model for regression estimates the reference value, as shown in Fig. 7, and the experimental results are summarized in Table VI. By calculating the correlation between the reference and estimated values, we confirmed that the model reasonably estimated the reference labeled by the expert. Thus, the features extracted using m-FIRS can be used to measure the DBs for MS and ME using an MLP model.

IV. DISCUSSION

Stimulation of muscles using an electrical stimulation generator causes involuntary muscle contraction. The IRS contains biomedical information regarding the DB/MS and DB/ME. A strong correlation between the extracted features and the reference was confirmed in this experiment. The proposed algorithm can robustly measure DBs using a feature vector extracted from the IRS.

Therefore, the proposed algorithm objectively measures DB/MS and DB/ME using the IRS. These results may reflect the general health status of the patients. The measurements can be conducted at home using a portable digital device called ExoRehab. We expect that intrinsic muscle diseases can be detected using long-term DB monitoring. We also propose the use of a DB and its feature vector for the diagnosis of myopathy. Moreover, we expect that it will be used to

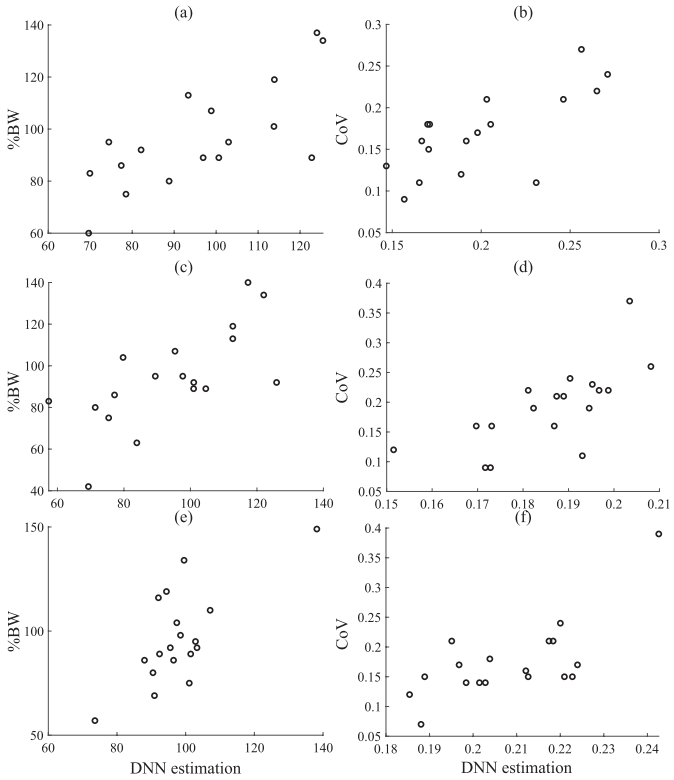

Fig. 7. Experimental results for the regression model based on the MLP. (a) Experimental results for the DB/MS in the set1 database. (b) Experimental results for the DB/ME in the set1 database. (c) Experimental results for the DB/MS in the set2 database. (d) Experimental results for the DB/ME in the set2 database. (e) Experimental results for the DB/MS in the set3 database. (f) Experimental results for the DB/ME in the set3 database.

scientifically prove the effects of digital medicine, such as digital therapeutics.

We proved that the bioinformatic characteristics within the IRS were related to muscle condition; therefore, we considered that patients with spinal muscular atrophy (SMA) and myopathy, as well as healthy elderly individual, could be classified using the IRS. Indeed, when our model estimated the DB using data from a few patients with SMA, it was confirmed that the DB of patients with SMA was distinctly separated from that of the elderly, who belong to the high-risk group of patients with myopathy. After collecting more data from patients with SMA and those with myopathy, we plan to extend the DB measurement technique to patients with SMA and myopathy. Based on the results of this study, we expect that the IRS of the DB can be used to classify muscle-related diseases and objectively estimate disease severity. Finally, because the DB technique is used to scientifically prove the current muscle condition of patients, the effects of drugs on muscle diseases can be proven. Thus, we expect that the DB technique can be used by patients to obtain insurance approval to obtain drugs at lower costs.

We observed various muscle properties through the m-FIRS recorded by the electrical stimulation set to 10–30 Hz for the frequency parameter. We did not set the electrical stimulation frequency above 35 Hz because the signal may not have been properly analyzed if the muscle was not sufficiently relaxed after a stimulated contraction. In the future, we may need to prove the effectiveness of m-FIRS at a higher frequency. In addition, when stimulating the muscle for each subject using the equivalent electrical stimulation, the IRS was recorded differently for each subject in accordance with the DB/MS and DB/ME. And, to obtain various information from the muscle, we analyzed the muscle with the diverse signal which consisted of multi-frequency IRS. For this, we preferentially carried out experiment through the IRS recorded by electrical stimulation of the designed frequency parameter (10-30 Hz, in 5 Hz increment) to confirm the feasibility of proposed system. And, in future, we plan to finely research the frequency parameter in order to improve performance of the proposed system. After we carry out the planned research, we expect that the hyper-parameter can be determined in terms of frequency of electrical stimulation in order to present best performance.

V. Conclusion

To measure the DB of the target muscle, the IRS was recorded using an EMG sensor while the muscle was stimulated using an electrical stimulation generator. We also collected the m-FIRS database for the subjects to analyze various biomedical characteristics, and the muscle response depended on the frequency of electrical stimulation. To do this, we extracted the feature vector to analyze the muscle condition, and the correlation between the features and reference was strong. Thus, when performing a performance evaluation using a test database that does not include a training database, the model can be used to robustly estimate the DB. In addition, we compared the MLP model with conventional methods, such as SVM, GMM, and ANN, to verify the performance of the proposed algorithm. The MLP model can estimate DBs more elaborately than the conventional method in terms of complex data; therefore, it performed better in measuring DB measurement.

Appendix A
Procedure for the Labeling of the Torque Data

1) We measured the torque data of the subject using torque equipment set to 60°/s.
2) The subject performed the leg-extension motion 10 times.
3) We measured the torque data of the subject using torque equipment set to 180°/s.
4) The subject performed the leg-extension motion 10 times.
5) An expert refined the torque data for labeling.
6) To evaluate the DB/MS, the peak torque of each motion in the 60°/s data was calculated, and then the %body weight (body weight, %body weight = peak torque/body weight) was extracted.
7) To evaluate the DB/ME, the average power of each motion in the 180°/s data was calculated, and the coefficient of variation (CoV) was extracted.
8) The weak and strong terms of the DB/MS and DB/ME were defined as follows:
   a) Strength-strong is defined by %body weight $\geq$ 100
   b) Strength-weak is defined by %body weight $<$ 100

c) Strength-strong is defined by CoV $<$ 0.17
d) Strength-weak is defined by CoV $\geq$ 0.17

9) To divide equivalently the number of data for each class, the threshold was determined as above.

REFERENCES

[1] S. Bulley et al., "Arterial smooth muscle cell PKD2 (TRPP1) channels regulate systemic blood pressure," *Neurosci. Phys. Living Syst.*, vol. 7, pp. 1–23, Dec. 2018.

[2] A. Dhingra et al., "Ellagic acid antagonizes Bnip3-mediated mitochondrial injury and necrotic cell death of cardiac myocytes," *Free Radical Biol. Med.*, vol. 112, pp. 411–422, Nov. 2017.

[3] N. A. Brazhe, E. I. Nikelshparg, C. Prats, F. Dela, and O. Sosnovtseva, "Raman probing of lipids, proteins, and mitochondria in skeletal myocytes: A case study on obesity," *J. Raman Spectrosc.*, vol. 48, no. 9, pp. 1158–1165, Jul. 2017.

[4] B. Bonnechère et al., "Automated functional upper limb evaluation of patients with friedreich ataxia using serious games rehabilitation exercises," *J. NeuroEng. Rehabil.*, vol. 15, no. 1, pp. 1–9, Oct. 2018.

[5] C. S. González-González, P. A. Toledo-Delgado, V. Muñoz-Cruz, and P. V. Torres-Carrion, "Serious games for rehabilitation: Gestural interaction in personalized gamified exercises through a recommender system," *J. Biomed. Informat.*, vol. 97, Sep. 2019, Art. no. 103266.

[6] J. Du et al., "Optimal electrical stimulation boosts stem cell therapy in nerve regeneration," *Biomaterials*, vol. 181, pp. 347–359, Oct. 2018.

[7] E. F. Hodkin et al., "Automated FES for upper limb rehabilitation following stroke and spinal cord injury," *IEEE Trans. Neural Syst. Rehabil. Eng.*, vol. 26, no. 5, pp. 1067–1074, May 2018.

[8] M. Jeon, M. O. Gu, and J. Yim, "Comparison of walking, muscle strength, balance, and fear of falling between repeated fall group, one-time fall group, and nonfall group of the elderly receiving home care service," *Asian Nursing Res.*, vol. 11, no. 4, pp. 290–296, Dec. 2017.

[9] J. M. Porto, A. P. M. Nakaishi, L. M. Cangussu-Oliveira, R. C. F. Junior, S. B. Spilla, and D. C. C. D. Abreu, "Relationship between grip strength and global muscle strength in community-dwelling older people," *Arch. Gerontol. Geriatrics*, vol. 82, pp. 273–278, May 2019.

[10] T. B. Willingham, J. Melbourn, M. Moldavskiy, K. K. McCully, and D. Backus, "Effects of treadmill training on muscle oxidative capacity and endurance in people with multiple sclerosis with significant walking limitations," *Int. J. MS Care*, vol. 21, no. 4, pp. 166–172, Jul. 2019.

[11] F. M. Ivey, S. J. Prior, C. E. Hafer-Macko, L. I. Katzel, R. F. Macko, and A. S. Ryan, "Strength training for skeletal muscle endurance after stroke," *J. Stroke Cerebrovascular Diseases*, vol. 26, no. 4, pp. 787–794, Apr. 2017.

[12] B. M. Baroni, C. V. Ruas, J. B. Ribeiro-Alvares, and R. S. Pinto, "Hamstring-to-quadriceps torque ratios of professional male soccer players: A systematic review," *J. Strength Conditioning Res.*, vol. 34, no. 1, pp. 281–293, Jan. 2020.

[13] S. Fudickar, S. Hellmers, S. Lau, R. Diekmann, J. M. Bauer, and A. Hein, "Measurement system for unsupervised standardized assessment of timed 'Up & Go' and five times sit to stand test in the community—A validity study," *Sensors*, vol. 20, no. 10, p. 2824, May 2020.

[14] A. Ibrahim, D. K. A. Singh, and S. Shahar, "'Timed up and Go' test: Age, gender and cognitive impairment stratified normative values of older adults," *PLoS ONE*, vol. 12, no. 10, Oct. 2017, Art. no. e0185641.

[15] S. Romano Smith, G. Wood, G. Coyles, J. W. Roberts, and C. J. Wakefield, "The effect of action observation and motor imagery combinations on upper limb kinematics and EMG during dart-throwing," *Scandin. J. Med. Sci. Sports*, vol. 29, no. 12, pp. 1917–1929, Dec. 2019.

[16] A. Kurtoglu and N. Konar, "A comparison of some anthropometric and motor features of visually impaired students who play sports and those who do not play sports in schools for the visually impaired in Turkey," *Eur. J. Phys. Educ. Sport Sci.*, vol. 7, no. 1, pp. 56–68, May 2021.

[17] A. Harb and S. Kishner, "Modified Ashworth scale," *Stat Pearls*, May 2021.

[18] R. Merletti and D. Farina, *Surface Electromyography: Physiology, Engineering, and Applications*. Hoboken, NJ, USA: Wiley 2016.

[19] D. Christiansen, M. J. MacInnis, E. Zacharewicz, H. Xu, B. P. Frankish, and R. M. Murphy, "A fast, reliable and sample-sparing method to identify fibre types of single muscle fibres," *Sci. Rep.*, vol. 9, no. 1, pp. 1–10, Apr. 2019.

[20] A. R. Coggan and L. R. Peterson, "Dietary nitrate enhances the contractile properties of human skeletal muscle," *Exerc. Sport Sci. Rev.*, vol. 46, no. 4, pp. 254–261, Oct. 2018.

[21] O. Wendowski, Z. Redshaw, and G. Mutungi, "Dihydrotestosterone treatment rescues the decline in protein synthesis as a result of sarcopenia in isolated mouse skeletal muscle fibres," *J. Cachexia, Sarcopenia Muscle*, vol. 8, no. 1, pp. 48–56, Feb. 2017.

[22] J. Xiao and S. Tang, "Joint learning of binary classifiers and pairwise label correlations for multi-label image classification," in *Proc. IEEE Conf. Multimedia Inf. Process. Retr. (MIPR)*, Aug. 2020, pp. 25–30.

[23] Z. Wang et al., "The power of short-term load algorithm based on LSTM," in *Proc. IOP Conf. Earth Environ. Sci.*, vol. 453, Aug. 2020, pp. 21–23.

[24] H. Akoglu, "User's guide to correlation coefficients," *Turkish J. Emergency Med.*, vol. 18, no. 3, pp. 91–93, Sep. 2018.

[25] V. Kehri, R. Ingle, S. Pail, and R. N. Awale, "Analysis of facial EMG signal for emotion recognition using wavelet packet transform and SVM," *Adv. Intell. Syst. Comput.*, vol. 748, pp. 247–257, Aug. 2018.

[26] J. Ziegler, H. Gattringer, and A. Mueller, "Classification of gait phases based on bilateral EMG data using support vector machines," in *Proc. IEEE Int. Conf. Biomed. Robot. Biomechtron.*, Aug. 2018, pp. 978–983.

[27] S. Saranya, S. Poonguzhali, and S. Karunakaran, "Gaussian mixture model based clustering of manual muscle testing grades using surface electromyogram signals," *Phys. Eng. Sci. Med.*, vol. 43, no. 3, pp. 837–847, May 2020.

[28] S. Michieletto et al., "GMM-based single-joint angle estimation using EMG signals," *Adv. Intell. Syst. Comput.*, vol. 302, pp. 1173–1184, Jan. 2015.

[29] Z. Zhang, K. Yang, J. Qian, and L. Zhang, "Real-time surface EMG pattern recognition for hand gestures based on an artificial neural network," *Sensors*, vol. 19, no. 14, p. 3170, Jul. 2019.

[30] N. Nazmi, M. A. Rahman, S. I. Yamamoto, and S. Ahmad, "Walking gait event detection based on electromyography signals using artificial neural network," *Biomed. Signal. Process. Control.*, vol. 47, pp. 334–343, Jan. 2019.